Monthly Notices
of the
ROYAL ASTRONOMICAL SOCIETY

MNRAS **430,** 3010–3016 (2013)
Advance Access publication

doi:10.1093/mnras/stt107

Comparing gaseous and stellar orbits in a spiral potential

Gilberto C. Gómez,[1]★ Bárbara Pichardo[2] and Marco A. Martos[2]

[1]*Centro de Radioastronomía y Astrofísica, Universidad Nacional Autónoma de México, Apdo. Postal 3-72, Morelia Mich. 58089, Mexico*
[2]*Instituto de Astronomía, Universidad Nacional Autónoma de México, Apdo. Postal 70-264, Ciudad Universitaria, México D.F. 04510, Mexico*

Accepted 2013 January 16. Received 2013 January 14; in original form 2012 June 19

ABSTRACT

It is generally assumed that gas in a galactic disc follows non-self-intersecting periodic stellar orbits closely. In order to test this common assumption, we have performed magnetohydrodynamics (MHD) simulations of a galactic-like disc under the influence of a spiral galactic potential. We have also calculated the actual orbit of a gas parcel and compared it to stable periodic stellar orbits in the same galactic potential and position. We found that the gaseous orbits approach periodic stellar orbits far from the major orbital resonances only. Gas orbits initialized at a given galactocentric distance but at different azimuths can be different, and scattering is conspicuous at certain galactocentric radii. Also, in contrast to the stellar behaviour, near the 4:1 (or higher order) resonance the gas follows nearly circular orbits, with much shorter radial excursions than the stars. Also, since the gas does not settle into a steady state, the gaseous orbits do not necessarily close on themselves.

Key words: MHD – Galaxy: disc – Galaxy: kinematics and dynamics – Galaxy: structure – galaxies: spiral – galaxies: structure.

1 INTRODUCTION

Differences between stellar orbital dynamics and gas dynamics in disc galaxies play a fundamental role in the interpretation (or misinterpretation) of kinematics observations in order to deduce general physical properties of galaxies. One example (Gómez 2006) is that the inferred quantity of dark matter in galaxies can be affected by inconsistencies between the well-studied gas rotation curve and the relatively poorly studied stellar disc rotation curve.

Several observational and theoretical studies have been devoted to the investigation of the relationship between the gas streamlines and the corresponding stellar orbits. In particular, it is customary to identify the non-self-intersecting stable periodic orbits of a given astronomical system, with plausible regions for gas streams to settle (e.g. Kalnajs 1973; Simonson & Mader 1973; Lindblad 1974; Wielen 1974; Sanders & Huntley 1976; van der Kruit 1976; Vandervoort & Keene 1978; van Albada & Sanders 1982; Sanders, Teuben & van Albada 1983; Contopoulos et al. 1989; Athanassoula 1992a,b; Patsis et al. 1994, 2009; Piner, Stone & Teuben 1995; Englmaier & Gerhard 1997; Patsis, Grosbøl & Hiotelis 1997; England, Hunter & Contopoulos 2000; Vega-Beltrán et al. 2001; Regan & Teuben 2003).

From resonances emerge strong orbital families like the x1 type that manage to survive in models up to approximately the 4:1 resonance. After that periodic orbits from many families are found. This means that at resonances new families of periodic orbits start existing. At resonances we may encounter more than one family of periodic orbits (Contopoulos & Grosbøl 1986; Heller & Shlosman 1996; Kaufmann & Patsis 2005). This is in part intrinsic to the problem, due to the non-linear character of the perturbations. In normal non-barred spiral galaxies with a moderate non-axisymmetric component, such as spiral arms, the stellar orbits and gaseous flow can be highly non-linear (this means, the response of a dynamical system to a perturbation depends non-linearly on the amplitude of the perturbation), even far from resonances. Also, phenomena like gas shocks or stellar chaos are found even in the case of low-amplitude spiral perturbations (Pichardo et al. 2003; Pérez-Villegas et al. 2012).

Large-scale galactic gaseous and stellar flows present various important differences in their kinematics. Some interesting known differences between the response of gas and stars to an imposed galactic potential model are due to the fact that gas is very responsive and suffers violent shocks, unlike stars. In resonant regions, it has been suggested that shocks occur close to the intersections of stable periodic orbits (Schwarz 1981; van Albada & Sanders 1982; Athanassoula 1992b). Gas is attracted to the spiral arms by their gravitational field and, unlike stars, it responds to pressure gradients. In non-barred galaxies with large bulges or thick discs (such as early spirals), stars are supported not only by rotation but also by strong radial velocities or velocity dispersion, while gas settles down in much thinner discs supported by rotation. The later the morphological type of the galaxy, the more similar are gas and stellar kinematics (Beckman, Zurita & Vega Beltrán 2004).

In this work we study the interplay between gas flow and stellar orbital dynamical properties of spiral galaxies. We have calculated

★E-mail: g.gomez@crya.unam.mx

Table 1. Non-axisymmetric galactic model (Pichardo et al. 2003).

Parameter	Value	Reference
Spiral arms locus	Bi-symmetric (Logthm)	Churchwell et al. (2009)
Spiral arms pitch angle	15.°5	Drimmel (2000)
Spiral arms external limit	12 kpc	Drimmel (2000)
Spiral arms: exp. with scale-length	2.5 kpc	Disc based
Spiral arms force contrast	∼10 per cent	Patsis, Contopoulos & Grosbøl (1991)
Spiral arms pattern speed (Ω_P)	20 km s^{-1} kpc	Martos et al. (2004)

a set of magnetohydrodynamics (MHD) and particle simulations in a static background gravitational potential based on a full 3D spiral galactic model (Pichardo et al. 2003). This includes spiral arms different in nature to the classic tight winding approximation, in order to contribute to the understanding of the relationship between stellar orbits and gas orbits in non-barred spiral galaxies, and the relation with periodic orbits inside and outside resonance regions.

This paper is organized as follows. In Section 2, the galactic potential used to compute the MHD and stellar orbits and the initial simulation set-up is described. In Section 3, the stellar and MHD orbits obtained with the spiral potential are presented and compared with each other. In Section 4, we present a brief summary and discussion of our results.

2 NUMERICAL MODEL

For the purpose of this work we have produced MHD simulations under the effect of a detailed model of the background galactic potential. We describe next the potential model and the performed simulations.

2.1 The galactic background model

For the orbital study we have employed a detailed galactic semi-analytic model, resembling a Milky-Way-like potential. Rather than using a simple ad hoc model for a three-dimensional spiral perturbation (such as a cosine function), we constructed a three-dimensional mass distribution for the spiral arms and derive their gravitational potential and force fields from previously known results in potential theory. The spiral arms distribution consists of inhomogeneous oblate spheroids superposed along a given spiral locus. It is physically simple, with continuous derivatives and density laws. In principle, the dimensions and mass density of the oblate spheroids will depend on the type of spiral arms that are modelled, gaseous or stellar. The model, called PERLAS, is described in detail in Pichardo et al. (2003). Comparisons of the model with other models have been already published, in particular for the most relevant parts of our study, the spiral arms perturbation (Pichardo et al. 2003; Martos et al. 2004; Antoja et al. 2009). The corresponding observationally motivated parameters of the model used for this work are presented in Table 1. The spiral perturbation is a 3D steady two-armed model that traces the locus reported by Drimmel & Spergel (2001), using *K*-band observations. The solar radius, at 8.5 kpc, is close to the spiral arms 4:1 resonance. The mean force ratio between the arms and the axisymmetric background is around 10 per cent, which is in agreement with the estimations by Patsis et al. (1991) for Milky-Way-type galaxies. At the solar circle, the radial component of the force due to the spiral arms is 4.4 per cent of the mean axisymmetric background. The self-consistency of the spiral arms has been tested through the reinforcement of the spiral potential by the stable periodic orbits (Patsis et al. 1991; Pichardo et al. 2003).

2.2 The MHD set-up

The initial set-up of the MHD simulations consists of a gaseous disc with a density profile given by $n(r) = n_0 \exp[-(r - r_0)/r_d]$, where $n_0 = 1.1\,\mathrm{cm}^{-3}$, $r_0 = 8$ kpc and $r_d = 15$ kpc. The gas behaves isothermally with a temperature $T = 8000$ K and is permeated by a magnetic field, initially in the azimuthal direction, with intensity $B(r) = B_0 \exp[-(r - r_0)/r_B]$, where $B_0 = 5\,\mu$G and $r_B = 25$ kpc. The disc is initially in rotational equilibrium between the centrifugal force, the thermal and magnetic pressures, magnetic tension and a background axisymmetric galactic potential (Allen & Santillán 1991) consisting of a bulge, stellar disc and halo.

This equilibrium is perturbed by the PERLAS spiral arm potential, which rotates with a pattern speed of $\Omega_P = 20\,\mathrm{km\,s^{-1}\,kpc^{-1}}$. This pattern speed and background potential place the inner Lindblad, 4:1, corotation, −4:1 and outer Lindblad resonances at 2.81, 6.98, 10.92, 14.37 and 17.72 kpc, respectively.

We solved the MHD equations with the ZEUS code (Stone & Norman 1992a,b), which is a finite difference, time explicit, operator split, Eulerian code for ideal MHD. We used a 2D grid in cylindrical geometry, with $R \in [1.5, 22\,\mathrm{kpc}]$ and a full circle in the azimuthal coordinate, ϕ, using 750 × 1500 grid points. Both boundary conditions in the radial direction were outflowing. All calculations are performed in the spiral pattern reference frame. No self-gravity of the gas was considered.

The simulation starts with the gas in circular orbits in equilibrium with the background galactic potential, thermal and magnetic pressure gradients and magnetic tension. After the perturbation is activated, the gas very rapidly settles into a spiral pattern, with two arms (plus an oval-shaped ring)[1] inside the inner Lindblad resonance (ILR) and four arms outside, up to the 4:1 resonance (see Fig. 1). The inner pair of arms follows a ∼9° pitch angle, while the two pairs outside the ILR follow a ∼9° and ∼13° pitch angles; in contrast, the perturbing arm potential follows a 15.°5 pitch. The exact position and pitch angle of the gaseous spiral arms oscillate slightly around the above quoted values.

It is noticeable the presence of an MHD instability at corotation radius (further described in Martos, in preparation), which begins to develop 2.8 Gyr after the start of the simulation. This instability is present in a variety of simulations with different magnetic field intensities, and absent in purely hydrodynamical ones. With exception of this instability, absence of a magnetic field does not affect our conclusions.

Fig. 2 compares the imposed stellar density with the response gas density at a time 1 Gyr after the start of the simulation. The stellar density is obtained by taking the Laplacian of the potentials corresponding to the axisymmetric background disc and spiral

[1] This ring at $r < 2$ kpc falls in a region where the dynamics should be dominated by a galactic bar, which is not included in this work. Therefore, it is disregarded.

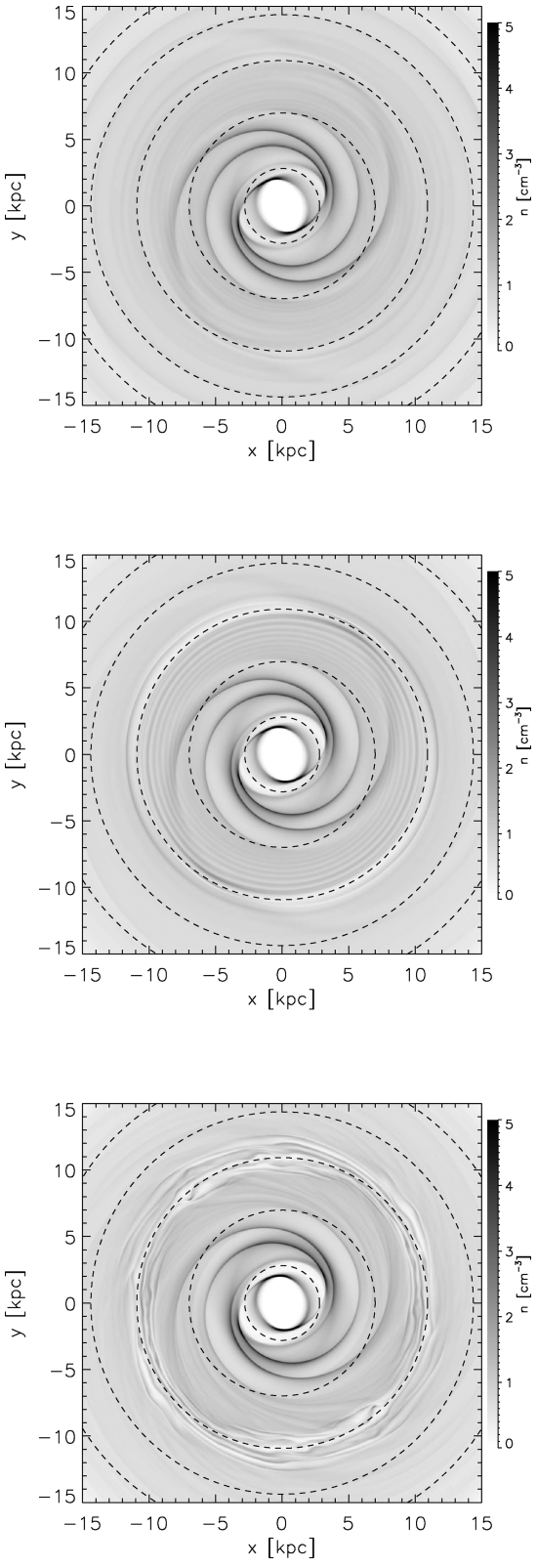

Figure 1. Density distribution after 1 Gyr (top), 2.5 Gyr (middle) and 4 Gyr (bottom). Although the computational grid extends to $r = 22$ kpc, only the inner region is shown. The dashed circles show the position of the inner Lindblad, 4:1, corotation, −4:1 and outer Lindblad resonances. Gas rotates in the clockwise direction (counterclockwise outside the corotation resonance).

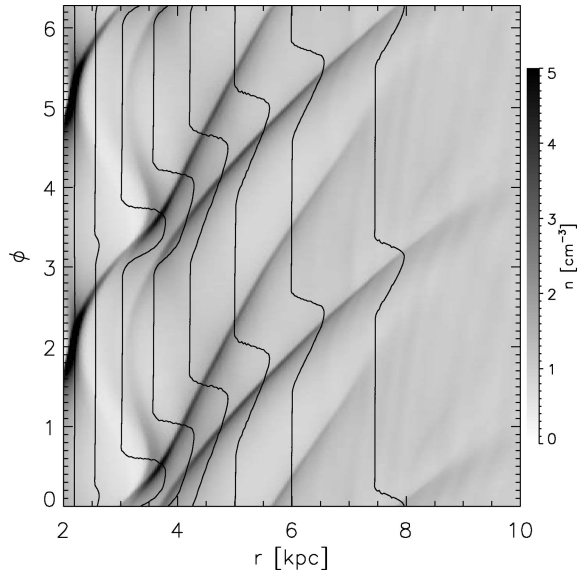

Figure 2. Comparison of the stellar (contours) and gaseous densities (grey-scale) in the simulation. The stellar density is that corresponding to the background axisymmetric galactic disc plus the (imposed) spiral arms potential, while the gas density corresponds to to that of a snapshot taken 1 Gyr after the start of the simulation. Since the model corresponds to a trailing spiral, the gas flows down from the top of the plot. The differences in number and position of the stellar and gaseous arms are apparent.

arm distribution, as given by the PERLAS model. In this figure, the differences in position and pitch of stellar and gaseous arms are apparent.

3 ORBITS IN THE SPIRAL POTENTIAL

Fig. 3 shows a comparison of stable periodic stellar and gaseous orbits in the background axisymmetric plus spiral galactic potential. This figure also shows the positions of the major resonances and

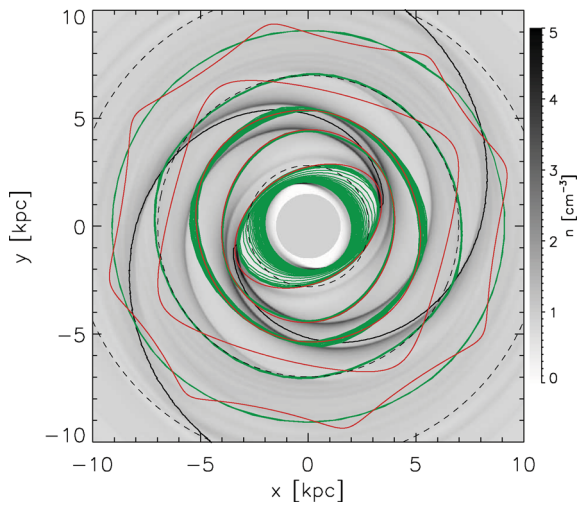

Figure 3. Comparison of some stellar (red) and gaseous (green) orbits near major resonances. The location of the ILR, 4:1 and corotation are indicated by dashed circles. The gaseous orbit near the ILR starts similar to the stellar orbit, but it rapidly decays to a ring. Around other resonances, the gas follows a near circular orbit, even as the stellar orbits experience large radial excursions. As reference, the gas density (grey-scale) and the locus of the stellar arms (black line) are also shown.

the locus of the spiral arms as defined in the PERLAS model. Since ZEUS is an Eulerian code, it does not provide the actual path a gas parcel follows. Therefore, in order to reconstruct a gaseous orbit, we integrated the velocity field interpolating in space and time between data files for an array of initial positions, following the trajectories of individual gas parcels in the resulting velocity field. The integration was performed over 4 Gyr, starting 1 Gyr into the simulation in order to avoid the initial settling of the gas into the spiral pattern. If during that time the gas parcel reaches either of the numerical boundaries (at $R = 1.5$ and 22 kpc), we stop the integration. The stellar orbits were obtained by direct integration in the potential, locating the periodic ones using a Newton–Raphson algorithm.

When comparing the stellar and gaseous orbits presented in Fig. 3, it is apparent that some of them are similar, but also some may be quite different, even when both gas and stars are subjected to the same gravitational potential.

Stars and gas follow orbits that are similar in the regions between the resonances. In Fig. 4, we show some of the orbits calculated

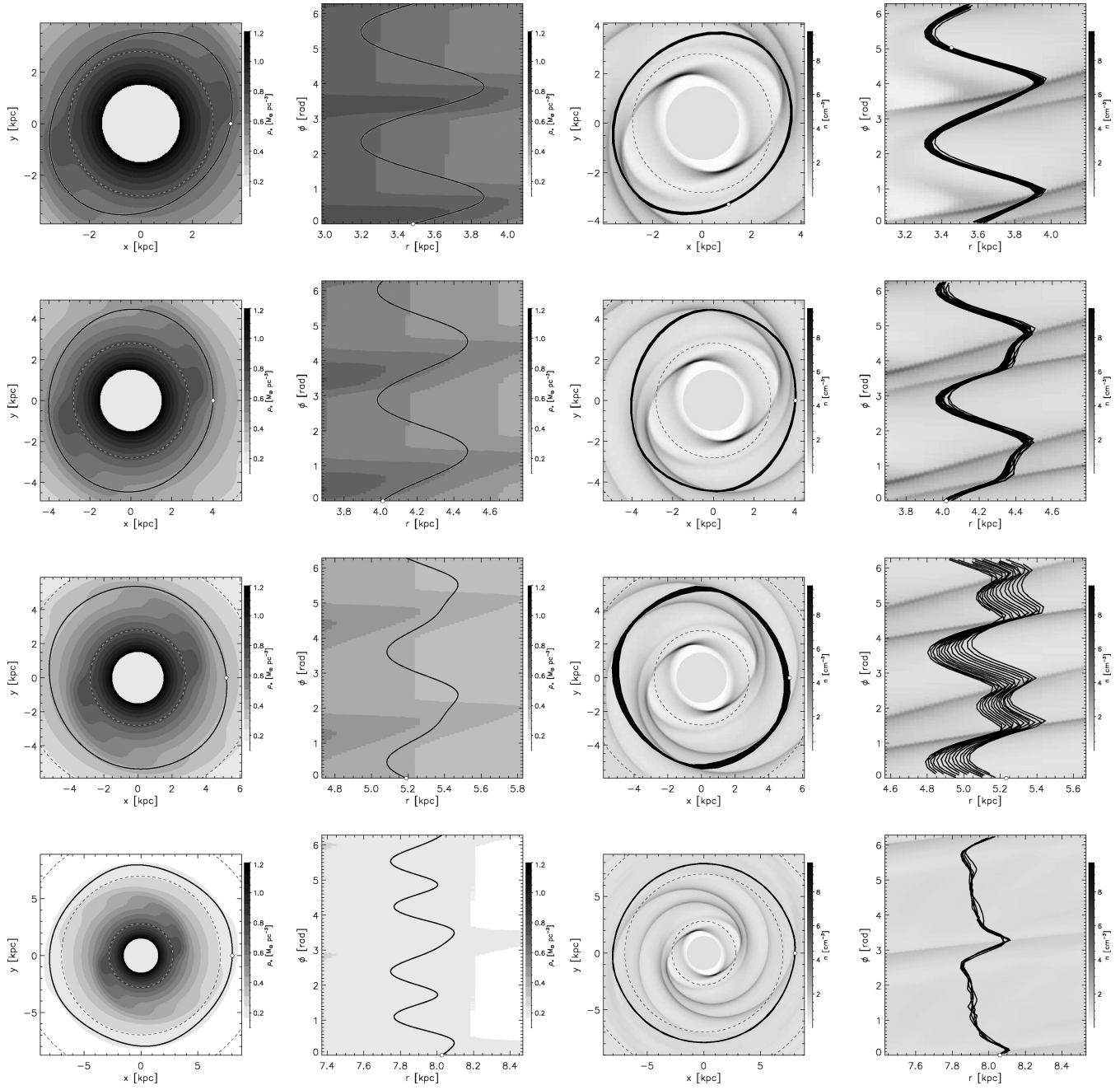

Figure 4. Comparison of stellar and gaseous orbits between resonances. The first two columns show stellar orbits in Cartesian (first column) and polar coordinates (second column) plotted over the stellar mass density (grey-scale) corresponding to the PERLAS potential model. The last two columns show gaseous orbits, also in Cartesian and polar coordinates, plotted over the gas density (grey-scale) averaged over the 4 Gyr period of the orbit integration. In all cases, the initial position of the integration is marked by the small open circle. Since the model corresponds to a trailing spiral, the sense of the gaseous orbits is clockwise in the Cartesian coordinate plots, and down from the top in the polar coordinate ones; only stellar orbits with the same sense of rotation were considered. The position of the inner Lindblad, 4:1 and corotation resonances is shown (dashed circles).

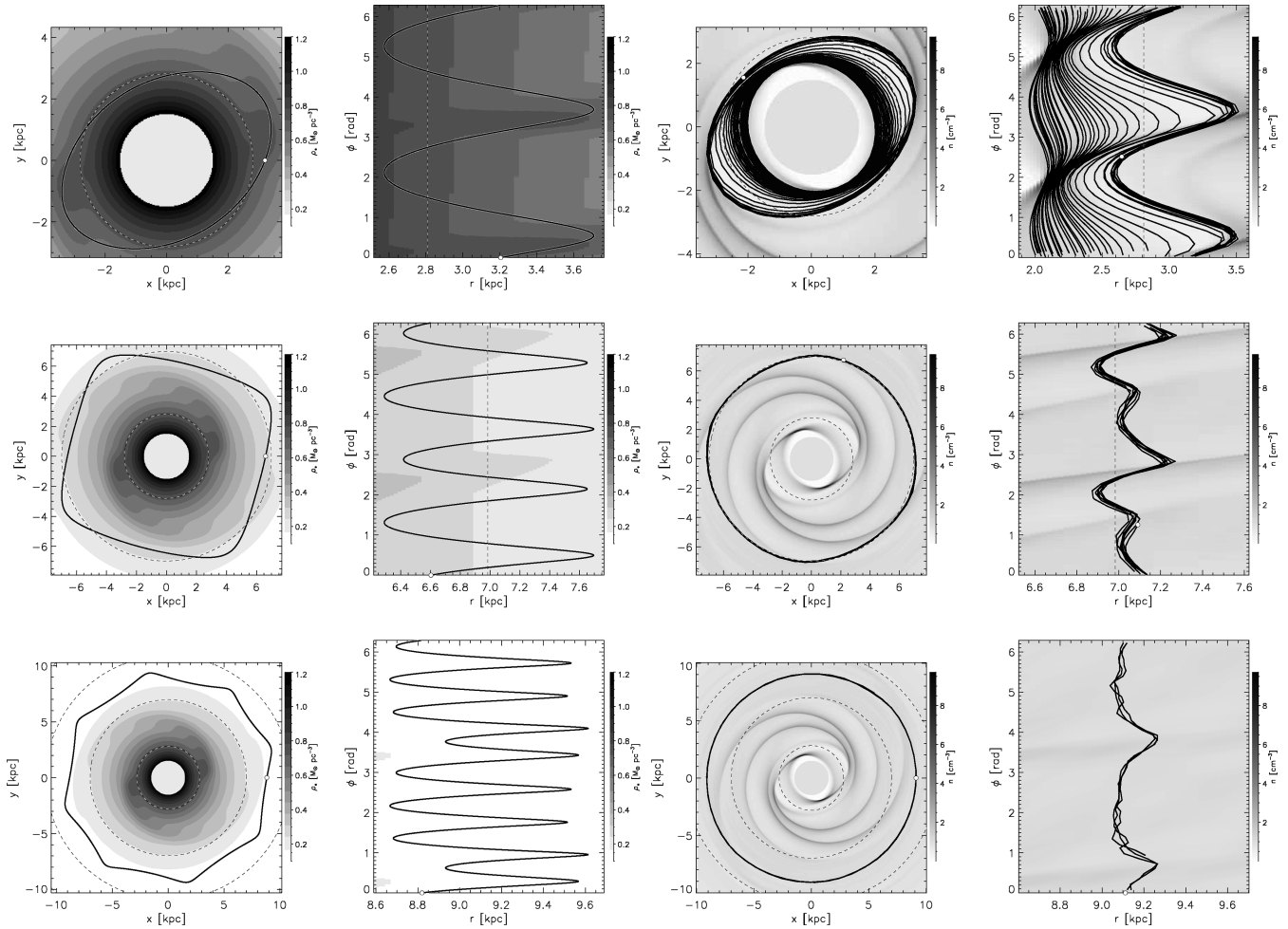

Figure 5. Similar to Fig. 4, for orbits near the resonances.

in similar regions; we also show the stellar mass and gas densities for comparison with the orbit. In the case of the stellar orbits, it is noticeable how the familiar oval shape (associated with the ILR) gradually morphs into a rounded square as the orbit approaches the 4:1 resonance. These last orbits are less supportive of the spiral pattern, in accordance with analytical theory.

Although the gas orbits are complex and quite sensitive to the initial position, they follow a similar evolution to the stars when regions away from the ILR are considered. It is noticeable that the gaseous orbits develop features that give rise to the second pair of spiral arms (apparent in the rightmost column of Fig. 4). As opposed to the stars, the gas may change direction rapidly by developing oblique shocks, which generate pressure gradients that further change the path of the orbit. Between the ILR and 4:1 resonance, the stellar and gaseous orbits are similar in the radial range they span, but the shape differs when the second pair of gaseous arms becomes stronger, since the shocks at the arm positions significantly change the path of the gas parcel. Just outside the 4:1 resonance, at the same Jacobi constant, we have more than one main family of periodic orbits coexisting, some of them stable, but the most of them unstable (see fig. 7 in Contopoulos & Grosbøl 1986). Most of stars approach an orbit with a fourfold symmetry; the gas, on the other hand, selects a twofold symmetric orbit related to the 2:1 coexisting periodic orbits family, associated with the only pair of arms found in the gas in this region.

Near the resonances, the gas and stars follow quite different orbits (Fig. 5). While the stars follow the familiar geometrical shapes, the gas is unable to follow the large departures from circularity of the stellar orbits. While the stars follow oval-shaped periodic orbits near the ILR, the gas actually tries to avoid that region. Integrations starting near or inside the ILR decay to the ring/spur structure just inside 2 kpc. This structure is not expected to appear in real galaxies, since usually it is affected by the starting position of the spiral arms and should be strongly influenced by a galactic bar not included in the present model. In fact, in order to find a gaseous orbit that resembles those found in the stars near the ILR, we must look for an orbit that remains outside the ILR region during its time evolution (the top row in Fig. 4, for example). Also, these gaseous orbits present some dispersion, since they are not quite periodic and actually cross themselves. This is possible since the simulation does not really reach a steady state, but instead settles on a periodic cycle, with the arms oscillating slightly around given positions.

Near the 4:1 resonance, the periodic stellar orbit follows the familiar rounded-square, while the gas actually remains close to a circular orbit, with deviations from circularity of less than 400 pc (although these deviations are systematic and allow for one pair of the gaseous spiral arms to extend beyond this resonance, as opposed to the stellar pattern). The strong evolution of the gaseous orbits around the ILR is absent near the 4:1 resonance.

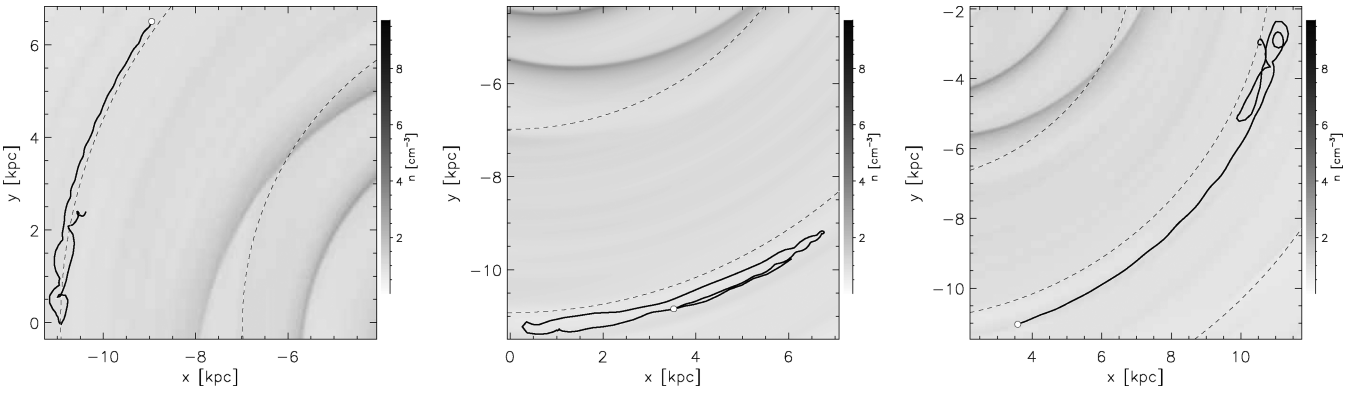

Figure 6. Gaseous orbits near the corotation resonance.

Further out, the expected banana-shaped orbits appear at some positions, although the gaseous orbits are greatly distorted due to the turbulence related to the instability at corotation (Fig. 6). The strong velocity perturbations related to this instability appear to generate points that act as attractors. Future work will try to determine whether these positions are suitable for star formation. Outside corotation, the gas orbits are nearly circular again, with deviations less than 0.5 kpc from the initial radius. This is not surprising since the underlying spiral perturbation is already weak, representing only 1 per cent of the radial axisymmetric force at the −4:1 resonance (the arm potential tapers-off at a radius of 12 kpc; see Pichardo et al. 2003).

4 DISCUSSION AND CONCLUSIONS

We performed MHD simulations of a gaseous disc subjected to the PERLAS spiral potential (disregarding the effect of a galactic bar, which will be explored in the future). We then studied the actual path the gas follows as it rotates around the galaxy in order to compare it with the stable periodic stellar orbits existing in that same galactic potential in order to test the frequently stated assumption that the gas should follow orbits close to the periodic stellar orbits that do not cross themselves. We found that the gas does not always behave that way.

The most obvious difference in the stellar and gas behaviour is that the gas responds to the two-arm potential with four spiral arms (Shu, Milione & Roberts 1973; Martos et al. 2004), organized in two pairs, each with a tighter pitch angle than the underlying potential. The four gaseous arms are well defined between the ILR and the 4:1 resonance, more or less straddling the stellar arms in similar fashion to the secondary compressions described by Shu et al. (1973) (see Fig. 2). Outside the 4:1 resonance, the gaseous arms follow the stellar arms more closely. The gas response to stellar arms depend on the details of the imposed potential (compare, for example, with Patsis et al. 1997; Vorobyov 2006) and will be explored in future work.

As opposed to stars, the gas may develop shocks at the arm positions, which allow its orbits (understood as the path a gas parcel follows) to change direction abruptly. This behaviour generates cusps in the gaseous orbits that are not present in the stellar orbits.

Setting aside the extra cusps in the gaseous orbits, the stellar and gaseous orbits are most similar in between the resonances, when the general shape and radial range are considered. These are the regions where the periodic stellar orbits are rounder and the radial excursions are smaller, allowing the gas to more closely follow the stellar orbits since it will be less influenced by forces other than gravity. Near the resonances, however, the stars suffer large radial excursions that imply regions with small curvature radii so that the orbit may close on itself (see Fig. 5). A gas parcel cannot follow such an orbit[2] and either loses angular momentum and moves away from the resonance (such as the orbit near the ILR), or settles in an orbit with only small radial excursions. The gravitational forcing that maintains the resonance is still present; so, even as the gas follows a nearly circular orbit, its velocity is not uniform, thus generating pressure waves that allow the spiral arm to extend across the resonant radius; this is apparent, for example, across the 4:1 resonance.

Although banana-type orbits should be present at the corotation radius, the gas only develops such orbits just beyond that resonance. Generally speaking, the gas experiences changes always in the outer side of the resonant radii, for example, the second pair of arms starts and end just outside the ILR and 4:1 resonance, respectively. This particular element will be further explored in future work.

When stating that the gas should follow stable periodic stellar orbits that do not cross, a key assumption is that the gas falls into a steady state. Small oscillations of the gaseous arms (an effect exacerbated when the vertical structure of the gaseous disc is considered; see Gómez & Cox 2004) and MHD instabilities (like that present at corotation; see Martos, in preparation) distort the gaseous orbits so that they may cross themselves. Other phenomena not considered here, like star formation and feedback, will further disrupt the path a gas parcel should follow.

On the other hand, in chaotic regions, such as the corotation zone, the phase space for stable periodic orbits is severely reduced. Gas dynamics behaviour in this region cannot be attributable to stable simple paths given by periodic orbits (Chatzopoulos, Patsis & Boily 2011). In these regions, chaotic stellar orbits might be the ones supporting large-scale structures, and gas might not be able to follow chaotic orbits since their trajectories are, in general, self-intersecting.

Since observations of the spiral structure of the Milky Way are well fitted by four arms in the gas and two in the stars, the orbits that support such structures cannot be the same. The differences in the orbital behaviour of gas and stars shown here highlights the difficulty of extrapolating the results of stellar dynamics to gas dynamics. Even if the motion is dominated by gravity, other physical processes may have a strong impact on the overall behaviour of a galactic disc.

[2] We have also found that there is a limit to the ellipticity of a 2:1 orbit (oval ones) at approximately 0.4, above which gas cannot settle down readily on the orbit because of the presence of strong shocks at the apocentre.

ACKNOWLEDGEMENTS

The authors wish to thank P. Patsis for useful discussions on the subject, W. Henney for reviewing the manuscript and an anonymous referee for comments that led to a much improved paper. This work has received financial support from UNAM-DGAPA PAPIIT grants IN106511 to GCG and IN110711 to BP.

REFERENCES

Allen C., Santillán A., 1991, Rev. Mex. Astron. Astrofis., 22, 255
Antoja T., Valenzuela O., Pichardo B., Moreno E., Figueras F., Fernández D., 2009, ApJ, 700, L78
Athanassoula E., 1992a, MNRAS, 259, 328
Athanassoula E., 1992b, MNRAS, 259, 345
Beckman J. E., Zurita A., Vega Beltrán J. C., 2004, in Ulla A., Manteiga M., eds, Lecture Notes and Essays in Astrophysics 1. Gallega de Mecanización, Vigo, p. 43
Chatzopoulos S., Patsis P. A., Boily C. M., 2011, MNRAS, 416, 479
Churchwell E. et al., 2009, PASP, 121, 213
Contopoulos G., Grosbøl P., 1986, A&A, 155, 11
Contopoulos G., Gottesman S. T., Hunter J. H., Jr, England M. N., 1989, ApJ, 343, 608
Drimmel R., 2000, A&A, 358, L13
Drimmel R., Spergerl D. V., 2001, ApJ, 556, 181
England M. N., Hunter J. H., Jr, Contopoulos G., 2000, ApJ, 540, 154
Englmaier P., Gerhard O., 1997, MNRAS, 287, 57
Gómez G. C., 2006, AJ, 132, 2376
Gómez G. C., Cox D. P., 2004, ApJ, 615, 744
Heller C. H., Shlosman I., 1996, ApJ, 471, 143
Kalnajs A. J., 1973, Proc. Astron. Soc. Aust., 2, 174
Kaufmann D. E., Patsis P. A., 2005, ApJ, 624, 693
Lindblad P. O., 1974, in Shakeshaft J. R., ed., Proc. IAU Symp. 58, The Formation and Dynamics of Galaxies. Kluwer, Dordrecht, p. 399
Martos M., Hernandez X., Yáñez M., Moreno E., Pichardo B., 2004, MNRAS, 350, 47
Patsis P. A., Contopoulos G., Grosbøl P., 1991, A&A, 243, 373
Patsis P. A., Hiotelis N., Contopoulos G., Grosbøl P., 1994, A&A, 286, 46
Patsis P. A., Grosbøl P., Hiotelis N., 1997, A&A, 323, 762
Patsis P. A., Kaufmann D. E., Gottesman S. T., Boonyasait V., 2009, MNRAS, 394, 142
Pérez-Villegas A., Pichardo B., Moreno E., Peimbert A., Velázquez H. M., 2012, ApJ, 745, L14
Pichardo B., Martos M., Moreno E., Espresate J., 2003, ApJ, 582, 230
Piner B. G., Stone J. M., Teuben P. J., 1995, ApJ, 449, 508
Regan M. W., Teuben P., 2003, ApJ, 582, 723
Sanders R. H., Huntley J. M., 1976, ApJ, 209, 53
Sanders R. H., Teuben P. J., van Albada G. D., 1983, in Athanassoula E., ed., Proc. IAU Symp. 100, Internal Kinematics and Dynamics of Galaxies. Reidel, Dordrecht, p. 221
Schwarz M. P., 1981, ApJ, 247, 77
Shu F. H., Milione V., Roberts W. W., Jr, 1973, ApJ, 183, 819
Simonson S. C., III, Mader G. L., 1973, A&A, 27, 337
Stone J. M., Norman M. L., 1992a, ApJS, 80, 753
Stone J. M., Norman M. L., 1992b, ApJS, 80, 791
van Albada T. S., Sanders R. H., 1982, MNRAS, 201, 303
van der Kruit P. C., 1976, A&A, 52, 85
Vandervoort P. O., Keene J., 1978, ApJS, 37, 519
Vega-Beltrán J. C., Pizzella A., Corsini E. M., Funes J. G., Zeilinger W. W., Beckman J. E., Bertola F., 2001, A&A, 374, 394
Vorobyov E. I., 2006, MNRAS, 370, 1046
Wielen R., 1974, PASP, 86, 341

This paper has been typeset from a TEX/LATEX file prepared by the author.